Mon. Not. R. Astron. Soc. **000**, 1–9 (2002) Printed 19 March 2011 (MN LATEX style file v2.2)

Diamagnetic Screening of the Magnetic Field in Accreting Neutron Stars II – The effect of polar cap widening

Sushan Konar[1⋆] and Arnab Rai Choudhuri[2]
[1]*Indian Institute of Technology, Kharagpur 721302, India*
[2]*Indian Institute of Science, Bangalore 560012, India*

ABSTRACT
Recently, we have proposed a model for the screening of the magnetic field of an accreting neutron star by the accreted material flowing from the polar regions towards the equator and sinking there underneath the surface (Choudhuri & Konar 2002). In this model it was assumed that the flow pattern remained stationary over time. However, as the surface magnetic field weakens, the accretion takes place over a wider region around the pole, making the flow more radial and isotropic. In the present work, we extend this two-dimensional model to include the time-dependence of the flow of the accreted material. The final radial flow is found to be less efficient in screening the magnetic field compared to the initial tangential flow. After an initial phase of rapid decay, the magnetic field slowly reaches an asymptotic value when the accretion becomes nearly isotropic and radial. Assuming the initial extent of the polar cap to be $\sim 5^0$–10^0, a simple geometric argument suggests that the magnetic field should decay by $3-4$ orders of magnitude before stabilizing to an asymptotic value, consistent with the magnetic fields observed in millisecond pulsars.

Key words: magnetic fields–stars: neutron–pulsars: general–binaries: general

1 INTRODUCTION

Observations suggest a connection between the low magnetic field of some neutron stars (binary/millisecond pulsars) and their being processed in binary systems, indicating an accretion-induced field decay in such cases. Radio pulsar data and their statistical analyses indicate that binary as well as millisecond and globular cluster pulsars, which almost always have a binary history and shorter spin periods, possess much lower field strengths, down to $\sim 10^8 G$ compared to the isolated pulsars which appear to have much larger magnetic fields ($\sim 10^{11} G$ – $10^{13} G$) and longer spin periods (see Lorimer (2001) and references therein). Evidently the accreting material induces a rapid dissipation of the magnetic field and also spins the neutron star up by bringing in additional angular momentum.

We do not have any *a priori* knowledge of the interior currents supporting the magnetic field of a neutron star. Depending on the generation mechanism, the field could either be supported by the crustal currents (Blandford, De Campli, & Königl 1979) or by the Abrikosov fluxoids of the proton superconductor in the stellar core. The evolution of the magnetic field in these two cases are expected to be different. Accordingly, two classes of models have been proposed for the evolution of the magnetic field in accreting neutron stars (see Bhattacharya (2002), Konar & Bhattacharya (2001) for brief reviews) - one relating the field evolution to the spin evolution and the other attributing the field evolution to direct effects of mass accretion. Evidently, the starting point for these models is to assume different kinds of initial field configurations.

Another possible method of field reduction is to screen it by the accreting material. As the highly conducting accreting plasma settles and spreads onto the surface of the neutron star, it could produce a diamagnetic screening effect, burying the stellar field underneath it. Interestingly, this mechanism would not depend on the location of the field in the stellar interior and would work irrespective of the nature of the interior currents. Though this mechanism was suggested quite early on (Bisnovatyi-Kogan & Komberg 1974; Taam & van den Heuvel 1986; Romani 1990; Romani 1995), it is only recently that the problem is being investigated in some quantitative detail.

It turns out that the accretion flow in the polar region of a magnetized neutron star is extremely sensitive to various magnetohydrodynamic instabilities and it is difficult to make even a qualitative assessment of the effectiveness of screening without a full three-dimensional computation which is yet to be attempted. A one-dimensional plane-parallel model by Cummings et al. (2001) has indicated that the diamagnetic screening is ineffective for field strengths above $\sim 10^{10} G$ as well as for accretion rates below $\sim 1\%$ of the local Eddington rate and at lower accretion rates the field can diffuse through the accreting matter. Recently, Melatos & Phinney (2001) have calculated the hydromagnetic structure of a neutron star accreting symmetrically at both the magnetic poles as a function of the accreted mass, starting from a polytropic sphere plus a centrally located magnetic dipole and have evolved the configuration through a quasi-static sequence of two-dimensional Grad-

⋆ E-mail: sushan@cts.iitkgp.ernet.in; arnab@physics.iisc.ernet.in

Shafranov equilibria with increasing accreted mass. They find that the accreted material spreads equator-ward under its own weight, compressing the magnetic field into a thin boundary layer and burying it everywhere except in a narrow, equatorial belt. According to their calculation the magnetic dipole moment scales as $B_0^{1.3}\dot{M}^{0.18}M_a^{1.3}$ where B_0, $\dot{M}$ and M_a are the initial field strength, the rate of accretion and the total accreted mass.

In an earlier work (Choudhuri & Konar (2002) - Paper I henceforth) we have presented a two-dimensional model to demonstrate the mechanism of diamagnetic screening. A neutron star with strong magnetic field undergoes polar-cap accretion. The material falling onto the polar cap flows horizontally along the surface towards the equator. The flows coming from the two polar caps meet near the equator and then sink below the surface. A subsurface poleward counter-flow is expected in the layers immediately beneath the surface layer of equator-ward flow. Deeper inside, the material settles radially onto the core. We obtained an analytical expression describing this flow in Paper I and studied the evolution of the magnetic field subject to such a flow, kinematically, using a numerical code. In the absence of magnetic buoyancy, we found that the magnetic field gets screened in the very short time scale of the surface flow. On the other hand, if magnetic buoyancy in the molten surface layers is included, the magnetic field is screened in the longer time scale of the interior flow. For a typical neutron star, these two time scales are estimated to be 1 year and 10^5 years respectively. As magnetic buoyancy is likely to be important, we concluded that the magnetic field would be screened in the longer time scale of 10^5 years.

Observations of millisecond and binary pulsars also indicate that their magnetic fields undergo little or no field reduction after the phase of active mass accretion is over. It is believed that the decaying magnetic field reaches an asymptotic value and then stops decaying any further. One of the limitations of Paper I has been that the calculations presented there threw no light on this aspect of the problem. We used a time-independent velocity field and consequently the magnetic field continued to decay indefinitely. In reality, the velocity field is expected to be highly time dependent. As the magnetic field becomes weaker and the magnetic pressure in the polar region drops, it is possible for the accreting material to flow through an increasingly larger region around the pole. In other words, the polar cap widens with time in an accreting neutron star. Eventually, the magnetic field becomes too small to be able to channelize the flow of the accreting material and the accretion becomes spherically symmetric. The aim of the present paper is to self-consistently incorporate this time dependence of the velocity field into the evolution of the magnetic field. We show that spherical accretion is less effective in screening a magnetic field compared to accretion through polar caps. Hence, as the polar cap widens and the accretion tends to be more isotropic, the screening of the magnetic field becomes less efficient and the decay of the magnetic field is arrested to a large extent. So, after an initial rapid decrease, the magnetic field reaches a phase of very slow decay thereafter. This result gives us a clue as to why the magnetic field of the neutron star attains an asymptotic value and does not decay any further.

It should be mentioned here that similar conclusions were drawn for the case of crustal currents undergoing accretion-induced ohmic dissipation (Konar & Bhattacharya 1997; Konar & Bhattacharya 1999a) where a purely spherical accretion was assumed to be operative at all times. In that case such behaviour of the magnetic field depends crucially on the nature of the detailed structural physics of the neutron star crust. The same scenario prevails even for a spin-down induced expelled flux subject to ohmic dissipation in the crust (Konar & Bhattacharya 1999b). These calculations augment the present work in which we trace the evolution of the magnetic field in the surface layers as the nature of the accretion changes with time. At later times, when the accretion becomes spherical the calculations presented in the earlier models would become relevant.

The layout of this paper is as follows. The mathematical formulation of the problem is presented in §2. In §3, we investigate the evolution of the magnetic field with time-independent flow, with different widths of the polar cap. In §4, we obtain the time evolution of the surface field with a time-varying flow pattern, adjusting itself to the change in the field strength. However, the results obtained in §4 are based on an assumption of the existence of a non-radial flow till very deep layers of the star, which is rather unphysical and serves only the purpose of demonstration. Therefore, in §5 we go on to look at the problem where the material flow is confined to a thin crustal region. There has been some disagreement regarding the flow pattern, first presented in Paper I, in particular about the presence of a reverse flow in the deeper layers. Therefore, in §6 we have demonstrated that the flow velocity proposed by us is quite general and incorporates flow velocity without a reverse flow as well and have compared our results with those obtained by using this kind of flow pattern. Finally, we summarize our conclusions in §7.

2 MATHEMATICAL FORMULATION

We follow the mathematical formulation developed in Paper I and present a brief summary here for the sake of completeness. The magnetic field of the neutron star evolves according to the induction equation:

$$\frac{\partial \mathbf{B}}{\partial t} = \nabla \times (\mathbf{v} \times \mathbf{B}) - \frac{c^2}{4\pi}\nabla \times (\frac{1}{\sigma}\nabla \times \mathbf{B}) \,, \tag{1}$$

where σ is the electrical conductivity of the medium (see, for example, Choudhuri (1998), Parker (1979)). Assuming an axisymmetric poloidal field, allowing us to represent the magnetic field in the form $\mathbf{B} = \nabla \times (A(r,\theta)\hat{\mathbf{e}_\phi})$, we find that A evolves according to the equation:

$$\frac{\partial A}{\partial t} + \frac{1}{s}(\mathbf{v}.\nabla)(sA) = \eta \left(\nabla^2 - \frac{1}{s^2}\right) A \,, \tag{2}$$

where $\eta = c^2/4\pi\sigma$ and $s = r\sin\theta$. Evidently, it is the poloidal component of $\mathbf{v}$ that affects the evolution of A. We integrate equation (2) subject to the following boundary conditions. The field lines from the two hemispheres should match smoothly at the equator, requiring $\partial A/\partial\theta = 0$ at $\theta = \pi/2$. To avoid a singularity at the pole, we should have $A = 0$ at $\theta = 0$. The magnetic field matches a potential field at the surface of the neutron star, whereas the lower boundary allows free advection of the field below. See Paper I for details of how these boundary condition are implemented.

Assuming a polar-cap accretion, we expect the material accumulated in the polar region to cause an equator-ward flow at the surface in both the hemispheres. We assume this flow to be confined in a shell which is primarily in the liquid part of the crust. Near the equator, the flows originating from the two polar regions meet, turn around and sink under the surface resulting in a poleward counter-flow immediately beneath the top layer. Eventually this material settles radially onto the core. It should be noted that the pole-ward counter-flow as well as the radially inward flow takes

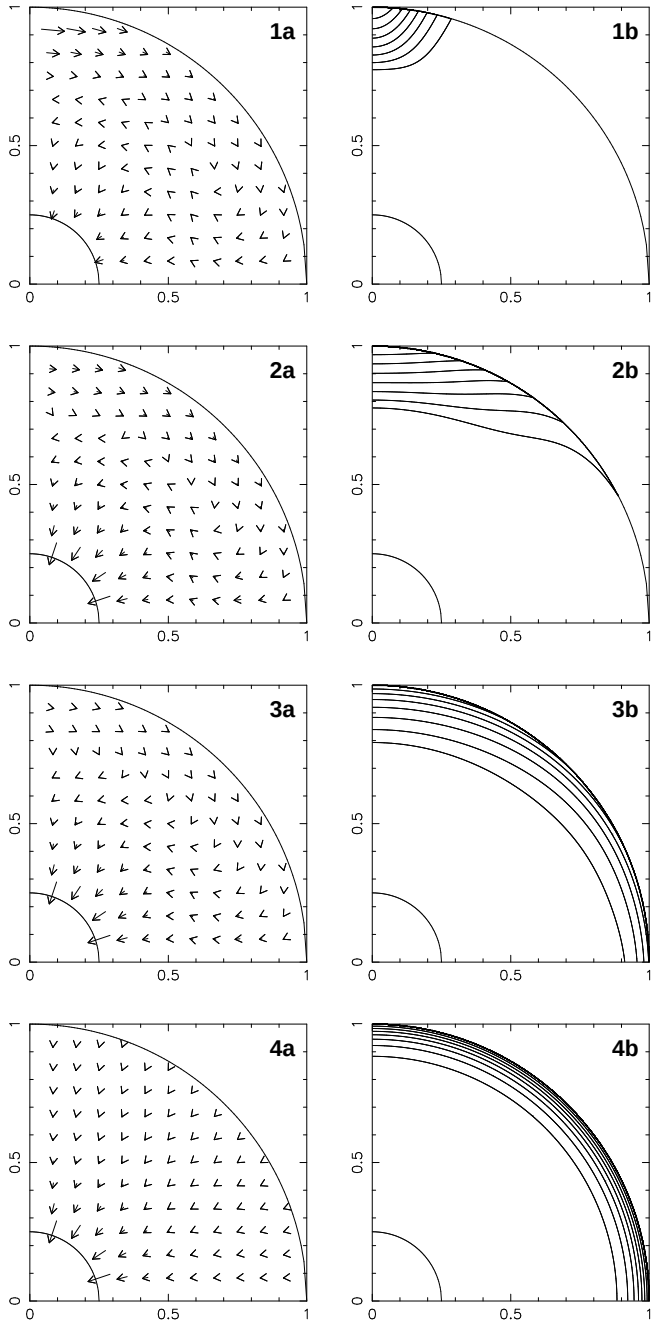

Figure 1. Flow velocity, $\rho\mathbf{v}$, and its divergence in a right-angular slice ($0 \leqslant \theta \leqslant \pi/2$, $0.25 \leqslant r \leqslant 1.0$). We have used $r_m = 0.75$, $r_b = 0.5$ for this picture. The panels marked $1a, 2a, 3a, 4a$ correspond to flow velocities with $c = 0.0, 0.25, 0.5, 1.0$ and the panels marked $1b, 2b, 3b, 4b$ are the divergences corresponding to those respectively.

place mainly in the solid crystalline region. The new material enters the region of interest only at the polar cap and therefore the flow-velocity has non-zero divergence only near the polar region. Apart from that $\nabla.(\rho\mathbf{v})$ should vanish everywhere else.

The analytic form of a velocity field, which has all the characteristics outlined above, is given below.

For $r_m < r < r_s$,

$$\rho v_r^{\mathbf{0}} = K_1 \left(\frac{1}{3}r - \frac{1}{2}r_m + \frac{\left(\frac{1}{2}r_m - \frac{1}{3}r_s\right) r_s^2}{r^2} \right) e^{-\beta \cos^2\theta}, \quad (3)$$

$$\rho v_\theta^{\mathbf{0}} = \frac{1}{2}\sqrt{\frac{\pi}{\beta}} K_1 \frac{(r - r_m)}{\sin\theta} \mathrm{erf}(\sqrt{\beta}\cos\theta) \left(1 - e^{-\gamma\theta^2}\right) . \quad (4)$$

For $r_b < r < r_m$,

$$\begin{aligned} \rho v_r^{\mathbf{0}} &= K_2\, e^{-\beta\cos^2\theta} \\ &\times \left(\frac{1}{3}r - \frac{1}{2}(r_m + r_b) + \frac{r_m r_b}{r} + \frac{\left(\frac{1}{6}r_b - \frac{1}{2}r_m\right) r_b^2}{r^2} \right) \\ &- \left(\frac{1}{3}r - \frac{1}{2}(r_m + r_b) + \frac{r_m r_b}{r} + \frac{\left(\frac{1}{6}r_m - \frac{1}{2}r_b\right) r_m^2}{r^2} \right) \\ &\times \frac{1}{2}\sqrt{\frac{\pi}{\beta}} K_2 , \end{aligned} \quad (5)$$

$$\begin{aligned} \rho v_\theta^{\mathbf{0}} &= \frac{K_2}{2\sin\theta}\sqrt{\frac{\pi}{\beta}} \left(r + \frac{r_m r_b}{r} - r_b - r_m \right) \\ &\times \left(\mathrm{erf}(\sqrt{\beta}\cos\theta) - \cos\theta \right) . \end{aligned} \quad (6)$$

For $r < r_b$,

$$\rho v_r^{\mathbf{0}} = -\frac{K_3}{r^2} , \quad (7)$$

$$\rho v_\theta^{\mathbf{0}} = 0 . \quad (8)$$

Notice that the parameter γ in $\mathbf{v}^{\mathbf{0}}(\beta, \gamma, r_b, r_m, r_s)$ defines the size of the polar cap, the angular extent being given by $\sim \gamma^{-1/2}$. Whereas, the parameter β determines the angular width of the down-flow that sinks inward below the equator. The flow is predominantly horizontal in the surface layer $r_m < r < r_s$. In the layer $r_b < r < r_m$ immediately below that, there is a pole-ward counter-flow. In this layer, the flow also tends to become more and more radial as it travels toward the deeper layers. Finally, below r_b, the material velocity becomes completely radial, flowing inward.

The flow in the innermost layers is nothing but the radial compression experienced by the deeper layers of the star due to an increase in the mass. Therefore, the magnitude of the velocity is related to the rate of accretion by the condition $K_3 = \dot{M}/4\pi$. Ensuring continuity across $r = r_m$ and $r = r_b$ we can relate K_1 and K_2 to K_3 and find that $\nabla.(\rho\mathbf{v}^{\mathbf{0}}) = 0$ everywhere below $r = r_m$. However, the divergence in the uppermost layer above $r = r_m$ is :

$$\begin{aligned} \nabla.(\rho\mathbf{v}^{\mathbf{0}}) &= K_1\, e^{-\gamma\theta^2 - \beta\cos^2\theta} \frac{r - r_m}{r} \\ &\times \left(1 + \sqrt{\frac{\pi}{\beta}} \frac{\gamma\theta}{\sin\theta} e^{\beta\cos^2\theta} \mathrm{Erf}(\sqrt{\beta}\cos\theta) \right) \end{aligned} \quad (9)$$

providing for a source of material only around the polar region in the upper layer. The panels $1a, 1b$ of Fig. 1 corresponds to this flow velocity and its divergence, defined above. (In Fig. 1 of Paper I we have shown this velocity field $\mathbf{v}^{\mathbf{0}}(\beta = 10.0, \gamma = 10.0, r_m = 0.75, r_b = 0.5)$ and its divergence $\nabla.(\rho\mathbf{v}^{\mathbf{0}})$. Please note that there is a typographical error in Paper I, where the values of both β and γ are mistakenly given as 1.0 instead of 10.0.).

As the magnetic field in the polar region weakens due to screening, (a) the polar cap widens and (b) the velocity field tends to become more radial. Eventually, when the magnetic field is sufficiently weak, the accretion becomes isotropic and spherical instead of being polar, with the flow velocity becoming completely radial everywhere. We represent both of these effects through a single parameter c taking values within the range $(0, 1)$. A larger value of c implies a wider extent of the polar cap and a more radial inflow. The effect of the widening of the polar cap can be made self-consistent by relating γ and c in the following manner:

$$\gamma = (\theta_{\rm min} + c\Delta\theta)^{-2}. \quad (10)$$

Since $\gamma^{-1/2}$ gives the angular width of the polar cap, we can see that $c = 0$ corresponds to an angular width of $\sim \theta_{\rm min}$, whereas $c = 1$ corresponds to $\theta_{\rm min} + \Delta\theta$. In this work, we have assumed $\theta_{\rm min} = 0.2$ and $\Delta\theta = 1.4$ such that the polar cap angle has a range of $\sim 10^o - 90^o$. Through γ, the flow velocity $\mathbf{v}_0(\beta, \gamma, r_b, r_m, r_s)$ too depends implicitly on c. In order to make the flow velocity more isotropic with the widening of the polar cap, an isotropic part is added to the velocity field. Therefore, the expression for the velocity field, for a time-dependent magnetic field strength and hence a time-dependent polar cap area, is given by (only showing the dependence on c)

$$\mathbf{v} = (1 - c)\,\mathbf{v^0}\,(\gamma(c)) + c\mathbf{v^1}\,. \quad (11)$$

Here $\mathbf{v^1}$ is the purely isotropic part given by

$$\rho\mathbf{v^1} = -\frac{K_3}{r^2}\left(1 - \exp\left(5\frac{r_s - r}{r_s - r_m}\right)\right)\,. \quad (12)$$

It is evident that $\rho\mathbf{v^1}$ vanishes at the surface and reaches an asymptotic value of $-K_3/r^2$ somewhere beneath the surface. It should be noted here that we are concerned with velocities inside the neutron star and not with those with which the accreting material may hit the surface of the star (which is certainly not zero at the surface). As freshly-accreted material makes the new surface up, the original surface moves deeper down. The above expressions define the material flow with respect to the surface at any given instant of time. Note that equations 11 and 12 imply a radial velocity of $-K_3/r^2$ below $r = r_b$, which is independent of c. Thus the rate of inflow of material to the neutron star core (which is determined by $\dot{M}$ and is related to K_3) does not change with c.

Fig. 1 shows the velocity field and its divergence for different values of c. It can be seen that the polar cap (indicated by the region where $\nabla.(\rho\mathbf{v})$ is substantially different from zero, implying deposition of accreted material) becomes larger with increasing values of c and the flow velocity also becomes more isotropic. Finally, for $c = 1.0$, the velocity field becomes fully isotropic and radially inward everywhere.

We now discuss how c at a certain instant of time depends on the magnetic configuration at that instant. The structure of the magnetosphere around an accreting neutron star is a well-studied subject (see, for example, Shapiro & Teukolsky (1983)). The extent of the polar cap area is limited by open field lines on the surface of the star. The last open field line is the one that goes through the Alfvén radius, $r_{\rm A}$, in the equatorial plane. Therefore, using the equation for dipolar field lines, we have

$$\sin\theta_{\rm P} = \left(\frac{r_s}{r_{\rm A}}\right)^{1/2} \quad (13)$$

where $\theta_{\rm P}$ is the angle between the last open field line and the magnetic axis, and therefore, the angular extent of the polar cap. At the Alfvén radius of an accreting system, the ram pressure of the infalling material equals the pressure of the magnetic field. Now, the ram pressure at the Alfvén radius is

$$P_{\rm ram} = \frac{1}{2}\rho(r_{\rm A})V^2(r_{\rm A})\,, \quad (14)$$

where $\rho(r_{\rm A})$ is the density and $V(r_{\rm A})$ is the velocity of the accreting material at Alfvén radius. Assuming matter to be in approximately free fall, we have $V(r_{\rm A}) = (2GM/r_{\rm A})^{1/2}$. The density of accreting material at Alfvén radius is $\rho(r_{\rm A}) = \dot{M}/4\pi V(r_{\rm A})r_{\rm A}^2$. Since the field is dipolar in nature, the field strength at the Alfvén radius is given by

$$B(r_{\rm A}) = \left(\frac{r_s}{r_{\rm A}}\right)^3 B_s\,, \quad (15)$$

where B_s is the field strength at neutron star surface. Equating the ram pressure and the magnetic pressure, one obtains

$$r_{\rm A} \;=\; (2GM)^{-1/7} r_s^{12/7} B_s^{4/7} \dot{M}^{-2/7}\,. \quad (16)$$

Assuming the rate of accretion ($\dot{M}$) and other stellar parameters (r_s, M) to be constant, we then have the following relation between the angular extent of the polar cap and the surface field strength:

$$\sin\theta(t)_{\rm P} \propto B_s(t)^{-2/7}\,. \quad (17)$$

In our model, the velocity field automatically adjusts to the change in the extent of the polar cap through a variation in γ. It follows from equation (10) that the opening angle of the polar cap $\theta(t)_{\rm P}$, given by $\gamma^{-1/2}$, is

$$\theta(t)_{\rm P} = \theta_{\rm min} + c(t)\,\Delta\theta\,. \quad (18)$$

Assuming $\theta_{\rm min}$ to correspond to the initial surface value of the magnetic field $B_s(t = 0)$, it follows from equation (17) and equation (18) that

$$\frac{\sin(\theta_{\rm min} + c(t)\,\Delta\theta)}{\sin\theta_{\rm min}} = \left[\frac{B_s(t)}{B_s(t=0)}\right]^{-2/7}\,. \quad (19)$$

It may be noted that equation (19) is valid only during the phase of accretion when the opening angle increases with the weakening magnetic field. When $c(t)$ equals one the accretion is completely spherical implying the extent of the polar cap to be $\pi/2$. At this point, the value of $c(t)$ is frozen and no further dependence of the magnetic field is included in $c(t)$ and the flow velocity profile.

To obtain the evolution of the magnetic field with time, we solve equation (2) with the velocity field described above. This velocity field, in turn, depends on the strength of the magnetic field through the parameter c. In most of our calculations, we have included magnetic buoyancy in the manner prescribed in Paper I, i.e, by including a radially upward velocity in the top layer. It has already been mentioned in Paper I that the numerical program used for this work has been adopted from that developed in the context of solar MHD which formed the basis of several calculations involving solar magnetic fields (Dikpati & Choudhuri 1994; Dikpati & Choudhuri 1995; Choudhuri, Schussler, & Dikpati 1995; Choudhuri & Dikpati 1999; Nandy & Choudhuri 2001; Nandy & Choudhuri 2002). The details of the numerical scheme can be found in the Appendix of Paper I.

3 MODIFIED FLOW VELOCITY

Before investigating the evolution of the magnetic field for a time-dependent flow velocity (resulting from a time-dependent size of the polar cap), we look at some representative cases with steady flow patterns corresponding to different sizes of the polar cap. For this, we use the modified form of the material flow velocity given by equation (11). The results of this section give an indication as to how the variation in the flow pattern affects the evolution of the magnetic field.

As in Paper I, we take the radius of the neutron star to be the unit of length. The unit of time is then fixed by equating the constant K_3 in the expression of velocity to unity. Our previous estimate shows that the equator ward flow at the surface takes place only through a narrow layer of 100 m, which is $\sim 1\%$ of the stellar

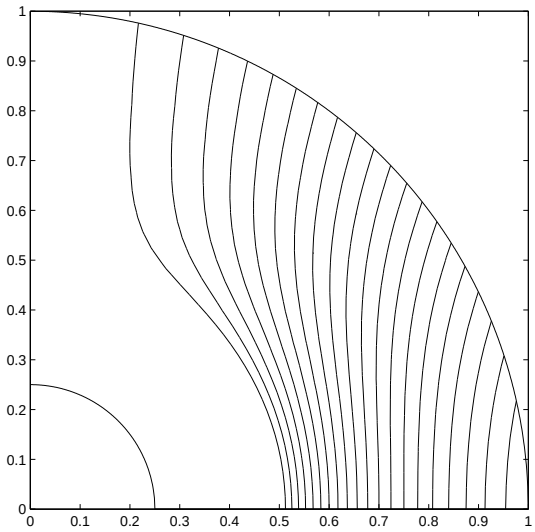

Figure 2. Initial field configuration, assuming a dipole confined to an outer region defined by $0.25 \leqslant r \leqslant 1$ and $0 \leqslant \theta \leqslant \pi/2$.

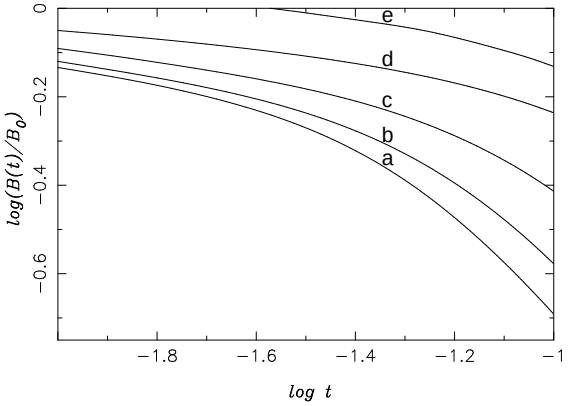

Figure 3. Evolution of the mid-latitude surface field with time. The curves a, b, c, d, e correspond to $c = 0.0, 0.25, 0.5, 0.75, 1.0$ respectively. $\eta = 0.05$ and $v_{\rm mb} = 50$ for all the curves.

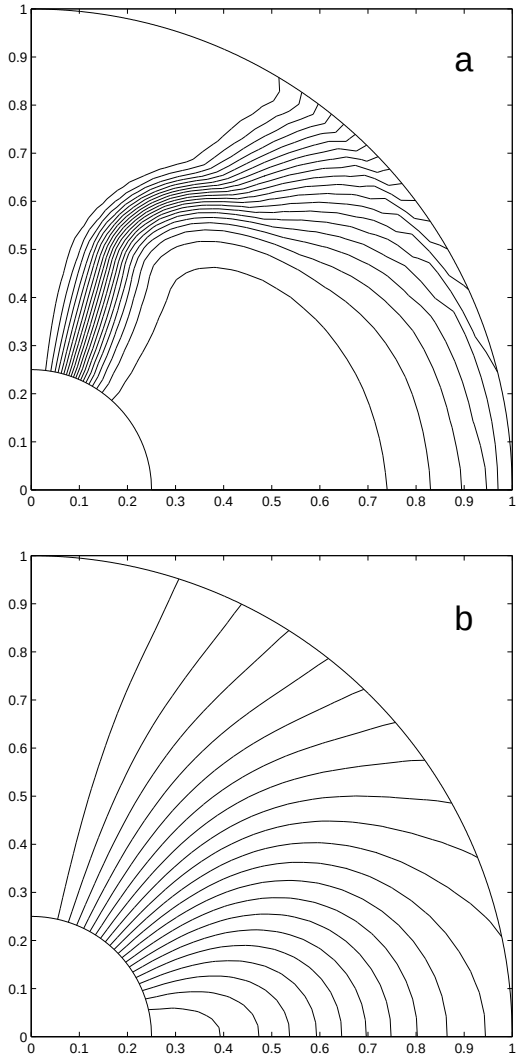

Figure 4. Field configuration at $t = 1.0$ starting from the initial configuration shown in Fig. 2. The panels marked a, b correspond to $c = 0.0, 1.0$ respectively (corresponding to the curves a and e of Fig. 3). In both the cases, $\eta = 0.05$ and $v_{\rm mb} = 50$ are assumed.

radius (Paper I). It is difficult to handle such a narrow layer in a numerical scheme. Moreover, it has been seen that most of the qualitative behaviour can be understood quite well by using a wider flow layer. Consequently, we have assumed $r_m = 0.75$, $r_b = 0.5$ for our calculations in this section and the next. Representative results with a narrow layer will be presented in §5. We take the diffusivity to be $\eta = 0.05$. As shown in Paper I, the magnetic field is more or less frozen in the fluid for this value of η and the results do not change on decreasing η any further. The parameter $v_{\rm mb}$ prescribing the magnetic buoyancy is set to the value 50.0. For all our calculations we assume β to be equal to 10.0.

We assume the initial currents to be entirely confined to the outer surface layers of the star and start with an initial magnetic field configuration shown in Fig. 2. This configuration is allowed to evolve in time with steady flow velocities corresponding to different sizes of the polar cap. The flow patterns for different extents of polar cap are obtained by taking different values of the parameter c (as depicted in the velocity fields shown in Fig. 1). Fig. 3 shows how the magnetic field at a point on the surface at the mid-latitude decays with time. It is clear that the decay slows down with increasing c, i.e. with increasing width of the polar cap. As the velocity field becomes more radial, it is less effective in screening the magnetic field. Fig. 4 shows the magnetic field configurations at time $t = 1.0$ for $c = 0$ and $c = 1.0$. It is evident that when c is zero, the effect of a reverse flow in the interior layers is quite prominent. Whereas, when c equals unity, i.e. the accretion is purely spherical, the field configuration shows only the effect of a radial compression. The fact that a more radial velocity field is less effective in screening the magnetic field, helps us to understand the results obtained with time-dependent velocity field more readily.

4 TIME-DEPENDENT FLOW VELOCITY

As accretion progresses, the magnetic field becomes weaker (due to screening, and also due to the ohmic dissipation in case of the crustal currents) and consequently the polar cap widens accord-

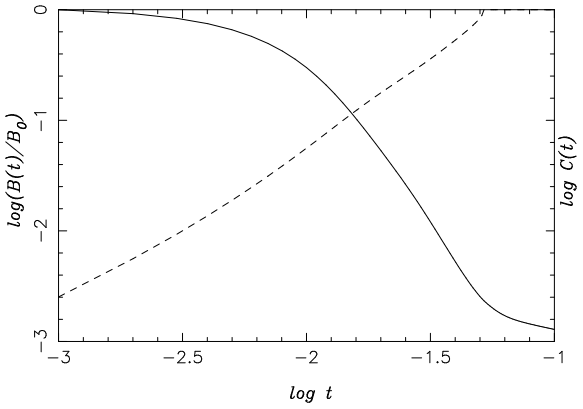

Figure 5. Evolution of the mid-latitude surface field with time for a time-dependent flow pattern (solid curve) with $\eta = 0.05$ and $v_{\rm mb} = 0$. The dashed curve shows the evolution of $c(t)$ with time.

ing to equation (17). This translates to equation (19) which gives the time-dependence of the parameter c, in terms of the time-dependence of the field strength at the surface.

Fig. 5 shows the evolution of the magnetic field at a point on the surface at the mid-latitude with time. It is clear that the decay slows down with time. As the polar cap widens out with time, the parameter c also increases. Since the magnetic field decay is slower for larger c, as we saw in the previous section, the evolution seen in Fig. 5 is quite expected. Fig. 6 shows the magnetic configurations at three instants of time, demonstrating the physical nature of the distortion and effective screening of the magnetic field. As expected from the results of the previous section, we see that gradually the field configuration shows the effect of a reverse interior flow less and less.

One of the important characteristics of binary and millisecond pulsars is that their surface field strength is weaker by a factor of about 10^3 – 10^4 compared to that of the normal pulsars. Therefore, it has been stressed that the magnetic field strength should reduce by such a factor during the phase of active accretion. We propose an extremely simple and elegant explanation for this effect. It is seen that the screening becomes much weaker after the accretion has become isotropic. Hence, effectively, the magnetic field decreases until it is weak enough for the polar cap to open up completely to 90^0 and then the field reduction slows down. It follows from equation (19) that the ratio of the initial to the final field strength should be of the order of $\sim (\sin 90^0/\sin\theta_{\rm min})^{7/2}$. Then, if $\theta_{\rm min}$ is about $5^0 - 10^0$, we obtain a factor of of 10^3 – 10^4 between the initial and the final surface field. Therefore, if the accretion onto a neutron star starts with a polar cap width of about $5^0 - 10^0$, the decrease in the magnetic field comes out to be of the right order of magnitude. For the case presented in Figs. 5 and 6, we have taken $\theta_{\rm min} = 0.2$ such that the factor $\sin^{-7/2}\theta_{\rm min}$ is $\sim 2.83 \times 10^2$. Notice that in Fig. 5 the magnetic field decays approximately by the logarithm of this factor (~ 2.45) before the decay essentially stops.

It should be noted here that the argument offered above does not account for the fact that the field decay continues via ohmic dissipation, if the currents reside in the crustal region, even after the accretion has become purely spherical (Konar & Bhattacharya 1997). Detailed modeling by (Konar & Bhattacharya 1999a) has shown that the ohmic dissipation is effectively stalled and the surface field strength reaches an asymptotic value only when material

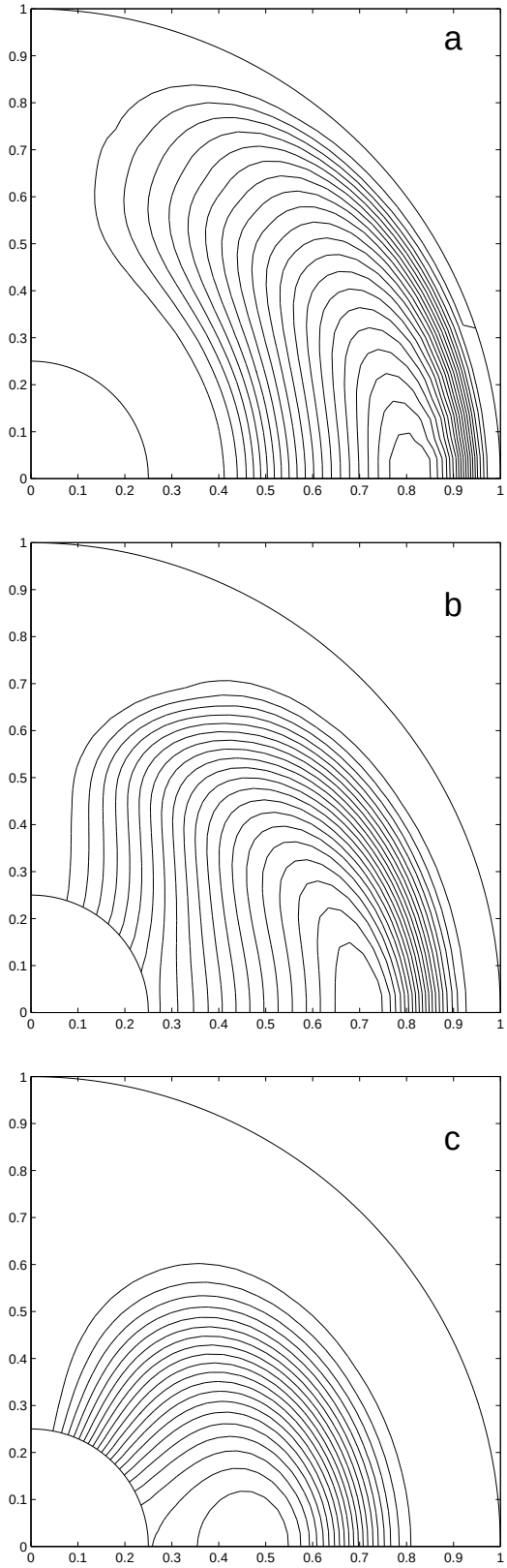

Figure 6. Field configuration at intermediate times starting from the initial configuration shown in Fig. 2. The panels marked a, b, c correspond to $t = 0.015, 0.05, 0.1$ respectively.

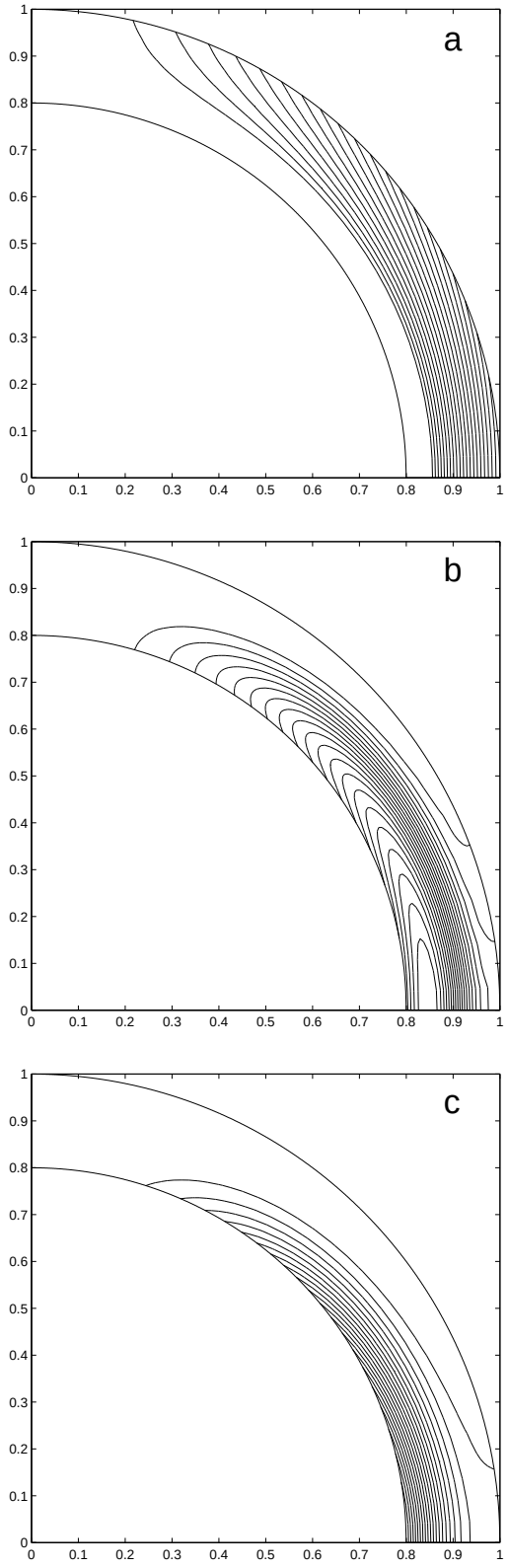

Figure 7. Field configuration at intermediate times starting from panel (a), confined to a region with $r \leqslant 0.8$ for $\eta = 0.05$ and $v_{\rm mb} = 50$. The panels marked b, c correspond to $t = 0.05, 0.1$ respectively.

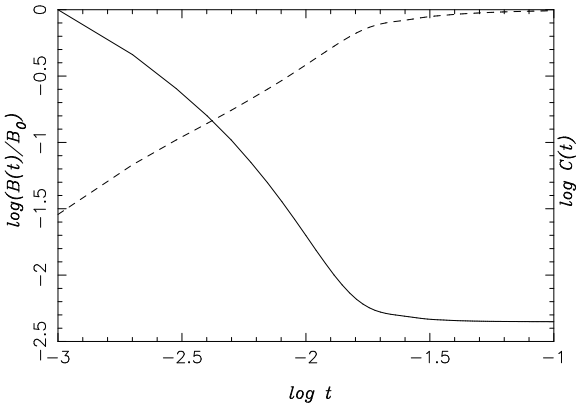

Figure 8. Evolution of the mid-latitude surface field with time for a time-independent flow pattern (solid curve). The initial field configuration is confined to a thin region as shown in the panel (a) of Fig. 7. $\eta = 0.05$ and $v_{\rm mb} = 50$ has been assumed here. The dashed curve shows the evolution of $c(t)$ with time.

of mass $\Delta M \sim 10^{-2}{\rm M}_\odot$ is accreted. Therefore, if the time-scales of the opening of the polar cap is comparable to that of the accretion of ΔM, the above argument would have a stronger claim to validity. However, a more detailed calculation of the screening process, taking into account the micro-physics of the neutron star crust, is required for a definite answer in this connection.

5 NARROW CRUSTAL REGION

It has already been mentioned that all our previous calculations are done by assuming the material flow happening in a wide subsurface region, with the bottom boundary at $r_b = 0.5$, than what is expected in reality. This is done for the ease of numerical calculation. However, in order to have an idea of the field evolution in such a narrow region here we reproduce some of the calculations of §4 confining the initial field configuration as well as the material flow in a region defined by $r_b = 0.90$ and $r_m = 0.95$, starting with an initial configuration shown in Fig. 7. But, it should be noted that in a real neutron star the flow region is confined to $r_m = 0.99$ which is beyond the viability limit of our numerical code.

Fig. 8 shows the evolution of the magnetic field at a point on the surface at the mid-latitude with time. It is clear that the decay is much faster compared to that in the situation where the flow happens in a much deeper region (Fig. 3). This is due to the fact that the distortion of the field lines occurs in a narrower region allowing for faster dissipation of the field through ohmic dissipation as can be interpreted from Fig. 7. Moreover, the field saturates at a value ~ 2.5 order of magnitude smaller than the original, which is about the same as what we see in Fig. 5. This lends credence to our argument that the field reduction basically depends on a geometric factor arising out of the polar cap opening and is independent of the depth of flow region. By extrapolating the results of this and the previous section, we expect that even in the case of a very narrow flow region appropriate for a neutron star, the magnetic field would first decay rapidly by a factor similar to what we have found above and would then saturate to an asymptotic value.

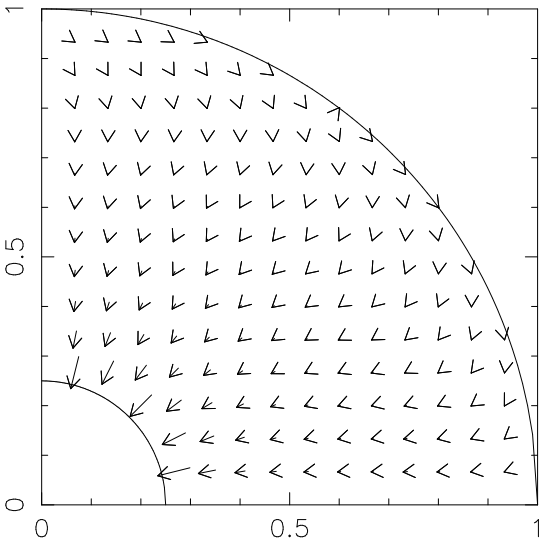

Figure 9. Material velocity without a region of interior reverse flow.

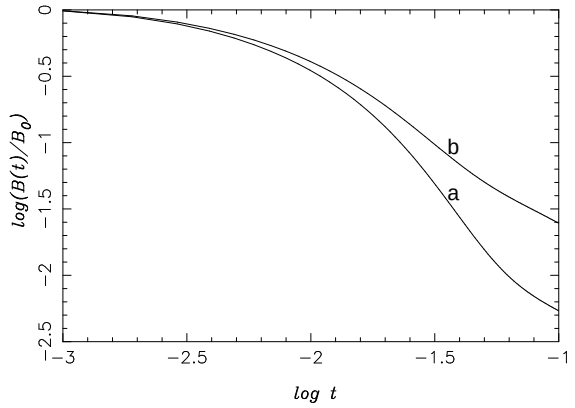

Figure 10. Evolution of the mid-latitude surface field with time for a time-independent flow pattern. The curves marked a, b correspond to a material movement with and without (Fig. 9) a reverse flow. $\eta = 0.05$ and $v_{\rm mb} = 0$ has been assumed for both the cases.

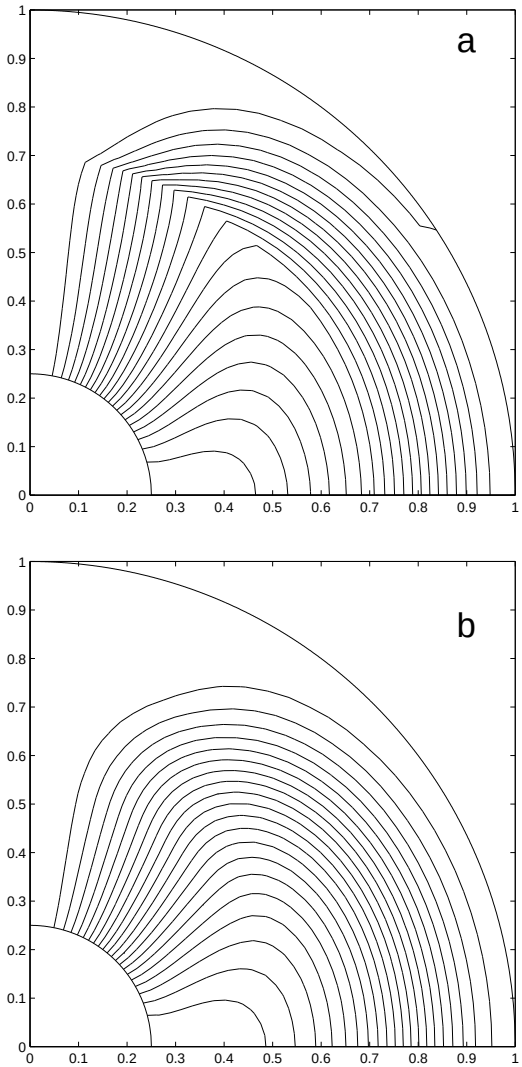

Figure 11. Internal field configuration at $t = 0.1$ starting from the initial configuration shown in Fig. 2. The panel marked a corresponds to the velocity without a reverse flow shown in Fig. 9 whereas the configuration in panel b has been evolved with a velocity pattern with a reverse flow (panel $1a$ of Fig.1).

6 VELOCITY WITHOUT COUNTERFLOW

It needs to be mentioned here that there is no clear consensus regarding the nature of the material flow. Many are of the opinion that there should be no counterflow and the flow in the surface layer should smoothly go over to a radial flow in the inner region (Geppert U., Konenkov D., Spruit H. C., *private communication*). The analytical form of the flow velocity, proposed by us, encompasses this possibility too. In the limit of $r_m \rightarrow r_b$ the flow takes this particular form as can be seen from Fig. 9.

Fig. 10 shows the evolution of the magnetic field at a point on the surface at the mid-latitude with time. Comparing the case without a counterflow to the case with such a counterflow, it is evident that the decay is slower in the first case. Since, in absence of a counterflow in the region immediately beneath the surface layer, the stretching and the subsequent distortion in the magnetic field is less, the effective decrease in the surface field strength is also expected to be smaller than in the case with a counterflow present. Moreover, as can be seen in Fig. 11, a flow pattern without an intermediate region of counterflow seem to give rise to a sharp bunching in the internal field configuration characteristic of the region in which the tangential surface flow changes over to a radial flow. This kind of bunching may perhaps lead to a faster dissipation of the currents at later times which we have not investigated at present. To sum up, the evolution of the magnetic field is qualitatively similar even when there is no counterflow, although the factor by which the magnetic field decreases is somewhat smaller.

7 CONCLUSIONS

Many of the questions regarding the screening of the surface magnetic field of a neutron star still remain unanswered. We have tried to address this issue by presenting the first two-dimensional analysis of the problem. In our previous work, we have considered a steady flow pattern. In the present paper, we extend this to encompass the more realistic case of the accretion flow becoming more

and more spherical with a reduction in the surface field strength. Therefore, with this work, the mathematical formulation of the problem can be said to be complete. However, a more detailed investigation of this problem incorporating the internal structure and the micro-physics of the neutron star crust is needed, and we expect to present the results of that investigation in a future communication (Konar 2003).

The main conclusion of this work is that the diamagnetic screening of the surface magnetic field becomes progressively less effective with time. As the strength of the surface field decreases due to screening, the magnetic field is less efficient in channeling the material flow and the accretion becomes more and more radial. Such radial in-fall of matter does not drag and bury the field lines unlike in the case of a horizontal flow. This fact is borne out by our calculations, and it is seen that the decay effectively stops after the polar cap has fully opened up. We estimate that the screening by accreting material should reduce the field by a geometric factor of about $\sim 10^3 - 10^4$ reaching an asymptotic value thereafter. Happily, these numbers match with what is observed in binary and millisecond pulsars (compared to the field strength in normal pulsars), providing motivation for further investigations in this direction.

ACKNOWLEDGMENTS

We would like to thank U. R. M. E. Geppert, Dennis Konenkov and H. Spruit for suggesting the alternative form of the velocity field. Both of us wish to thank IUCAA, Pune, where much of this work was carried out when SK was a post-doctoral fellow there and ARC was a senior associate.

REFERENCES

Bhattacharya D., 2002, Journal of Astrophysics and Astronomy, 22, 67
Bisnovatyi-Kogan G. S., Komberg B. V., 1974, Soviet Astronomy, 18, 217
Blandford R. D., De Campli W. M., Königl A., 1979, BAAS, 11, 703
Choudhuri A. R., 1998, The Physics of Fluids and Plasmas: An Introduction for Astrophysicist. Cambridge University Press
Choudhuri A. R., Dikpati M., 1999, Sol. Phys., 184, 61
Choudhuri A. R., Konar S., 2002, MNRAS, 332, 933
Choudhuri A. R., Schussler M., Dikpati M., 1995, A&A, 303, L29
Cumming A., Zweibel E., Bildsten L., 2001, ApJ, 557, 958
Dikpati M., Choudhuri A. R., 1994, A&A, 291, 975
Dikpati M., Choudhuri A. R., 1995, Sol. Phys., 161, 9
Konar S., 2003, in preparation
Konar S., Bhattacharya D., 1997, MNRAS, 284, 311
Konar S., Bhattacharya D., 1999a, MNRAS, 303, 588
Konar S., Bhattacharya D., 1999b, MNRAS, 308, 795
Konar S., Bhattacharya D., 2001, in The Neutron Star - Black Hole Connection, p. 71
Lorimer D. R., 2001, Living Reviews in Relativity, 4, 5
Melatos A., Phinney E. S., 2001, Publications of the Astronomical Society of Australia, 18, 421
Nandy D., Choudhuri A. R., 2001, ApJ, 551, 576
Nandy D., Choudhuri A. R., 2002, Science, 296, 1671
Parker E. N., 1979, Cosmological Magnetic Fields. Clarendon Press
Romani R. W., 1990, Nat, 347, 741
Romani R. W., 1995, in van Riper K., Epstein R., Ho C., ed, Isolated Pulsars. Cambridge University Press, p. 75
Shapiro S. L., Teukolsky S. A., 1983, Black Holes, White Dwarfs and Neutron Stars. John Wiley & Sons
Taam R. E., van den Heuvel E. P. J., 1986, ApJ, 305, 235

This paper has been typeset from a TEX/ LATEX file prepared by the author.